

Effect of spatial resolution on the estimates of the coherence length of excitons in quantum wells

M. M. Fogler,¹ Sen Yang,¹ A. T. Hammack,¹ L. V. Butov,¹ and A. C. Gossard²

¹*Department of Physics, University of California San Diego, La Jolla, California 92093*

²*Materials Department, University of California at Santa Barbara, Santa Barbara, California 93106*

(Dated: May 27, 2019)

We evaluate the effect of diffraction-limited resolution of the optical system on the estimates of the coherence length of 2D excitons deduced from the interferometric study of the exciton emission. The results are applied for refining our earlier estimates of the coherence length of a cold gas of indirect excitons in coupled quantum wells [S. Yang *et al.*, Phys. Rev. Lett. **97**, 187402(2006)]. We show that the apparent coherence length is well approximated by the quadratic sum of the actual exciton coherence length and the diffraction correction given by the conventional Abbe limit divided by π . In practice, accounting for diffraction is necessary only when the coherence length is smaller than about one wavelength. The earlier conclusions regarding the strong enhancement of the exciton coherence length at low temperatures remain intact.

PACS numbers: 78.67.-n,73.21.-b,71.35.-y

I. INTRODUCTION

A fundamental attribute of a quantum many-body system is its one-body density matrix

$$\rho(r) = \langle \Psi^\dagger(\mathbf{r}') \Psi(\mathbf{r}' + \mathbf{r}) \rangle, \quad (1)$$

where Ψ^\dagger (Ψ) are the particle creation (annihilation) operators and the averaging is done over both the quantum state and the position \mathbf{r}' (or equivalently, disorder). The density matrix is related to the momentum occupation function by the Fourier transform. It is also closely connected to other basic characteristics of the system: the spectral function and the single-particle propagator.¹

Normally, $\rho(r)$ decays with r as a result of scrambling the phases of the particles' wavefunctions by scattering and thermal fluctuations. The ratio

$$\xi_x = \left(\int_0^\infty \rho(r) r dr \right) / \left(\int_0^\infty \rho(r) dr \right) \quad (2)$$

gives the characteristic decay length of $\rho(r)$, which we refer to as the coherence length.

Since ξ_x provides a quantitative information about correlations, disorder, and interactions in the system, experimental techniques of measuring ξ_x are of much interest. They include, e.g., transport measurements (weak localization and the Aharonov-Bohm effect) and angle-resolved photoemission. The present paper concerns another, all optical method, which is suitable for excitons — bound states of electrons and holes in semiconductors. This technique was proposed in our recent paper,² where it was applied to the system of indirect excitons in GaAs coupled quantum wells.³ The motivation for studying the coherence length of indirect excitons is their ability to cool down to low temperatures, well below the temperature of quantum degeneracy, where a strong enhancement of ξ_x is anticipated.^{4,5} In this paper we refine the

estimates of the coherence length measured by our technique by taking into account the finite spatial resolution of the optical system.

Optical measurement of ξ_x is made possible by the fact that the coherence of excitons is imprinted on the coherence of the light they emit.^{6,7,8,9} The latter can be studied by the spatially resolved interferometry of the exciton photoluminescence (PL). In the aforementioned publication² this was accomplished as follows. The PL was collected from an area of size $D/M_1 = 2\text{--}10\ \mu\text{m}$ in the middle of one of the exciton beads¹⁰ ranging $\sim 30\ \mu\text{m}$ across. This was done by placing a pinhole of diameter $D = 10\text{--}50\ \mu\text{m}$ at the intermediate image plane of magnification $M_1 = 5$, see Fig. 1a. The light was then passed through a Mach-Zehnder (MZ) interferometer with a tunable delay length δl . The output of the interferometer was further magnified by the factor $M_2 \approx 1.6$ (so that the total magnification factor is $M = M_1 M_2$) and then

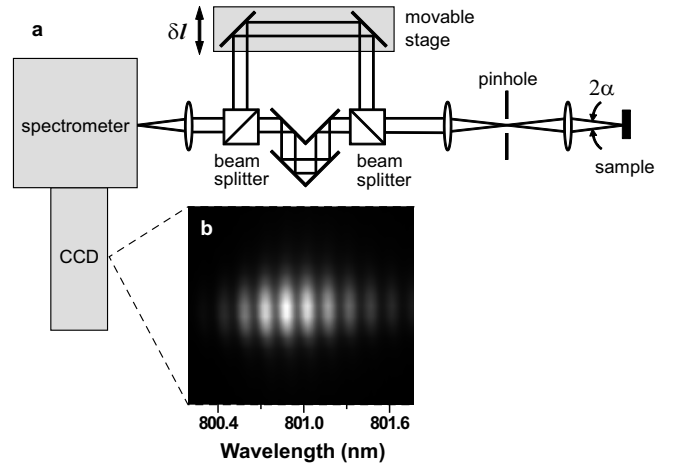


FIG. 1: (a) Experimental setup. The collection angle of the lens $2\alpha = 32^\circ$. (b) The interference pattern on the CCD for $D = 25\ \mu\text{m}$, $\delta l = 4.2\ \text{mm}$, and $T = 1.6\ \text{K}$.

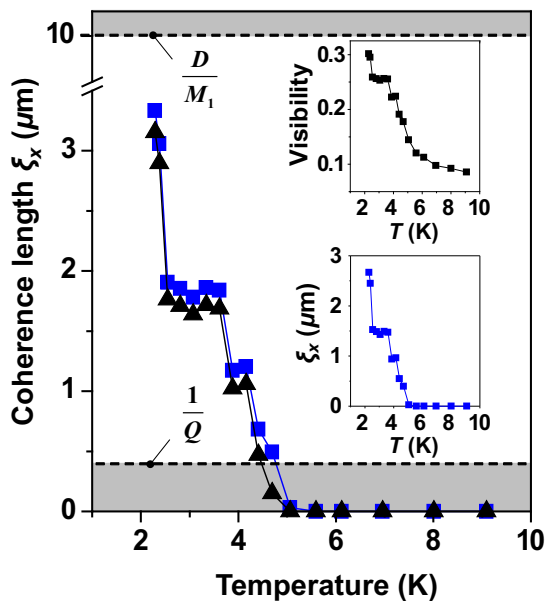


FIG. 2: Upper inset: function $V(T)$ measured in Ref. 2 for $D = 50 \mu\text{m}$ and $\delta l = 4.2 \text{mm}$. Main panel: ξ_x deduced from the fits of $V(T)$ to the theoretical curves in Fig. 3. The triangles (squares) are the estimates with (without) taking into account the spatial resolution of the experimental setup. The shaded areas are beyond experimental accuracy. Lower inset: previous estimates of the coherence length.¹¹

dispersed with a grating spectrometer, resulting in a periodically modulated interference pattern. The intensity $I = I(x)$ of this pattern was recorded by a CCD (Fig. 1b). Here x is the coordinate along the CCD image. Finally, a theoretical model that relates the visibility contrast, $V = (I_{\text{max}} - I_{\text{min}})/(I_{\text{max}} + I_{\text{min}})$ to ξ_x was used to analyze the data and determine ξ_x as a function of temperature.

The results of this approach are summarized in Fig. 2. As one can see, at $T < 4 \text{K}$ the exciton coherence length grows to a few μm , which exceeds the thermal de Broglie wavelength

$$\lambda_{\text{dB}} = \left(\frac{2\pi\hbar^2}{mk_B T} \right)^{1/2} \quad (3)$$

by an order of magnitude ($\lambda_{\text{dB}} \sim 0.1 \mu\text{m}$ at $T = 2 \text{K}$). Here $m = 0.2$ is the exciton mass in the quantum well in units of the bare electron mass. The inequality $\xi_x \gg \lambda_{\text{dB}}$ is anticipated for an exciton system near the superfluid transition. The conventional estimate of the transition temperature^{4,12,13} $T_{\text{BKT}} \sim (\hbar^2/m)(n/g)$ gives a few degrees K for the exciton concentrations¹⁴ $n/g \sim 10^{10} \text{cm}^{-2}$ ($g = 4$ is the spin degeneracy).

Our theoretical model of Ref. 2 used an approximation of geometrical optics for describing the light collection in the apparatus. This is justified in the most interesting regime of low T where ξ_x is large. On the other hand, at the upper end of the temperature range shown in Fig. 2 the estimated coherence length ξ_x was comparable with the diffraction-limited resolution of the optical system.

In particular, it was close to the Abbe limit^{15,16}

$$\text{Ab} = \frac{\lambda_0}{2\text{NA}}, \quad (4)$$

where $\text{NA} = \sin \alpha$ is the numerical aperture and λ_0 is the wavelength. The Abbe limit is not a “hard” limit but simply a characteristic measure of the optical resolution. In fact, another commonly used formulas due to Rayleigh^{17,18} differ from Eq. (4) by numerical factors. In this paper we study how the finite spatial resolution affects our earlier estimates of ξ_x and determine the appropriate numerical factors involved.

Our main result is as follows. Under certain assumptions, ξ_x is related to the *optical* coherence length ξ by

$$\xi = \sqrt{\xi_x^2 + \frac{1}{Q^2}}, \quad \frac{1}{Q} = \frac{\lambda_0}{2\pi\text{NA}}. \quad (5)$$

Here, in analogy to Eq. (2), ξ is defined by

$$\xi = \frac{1}{M} \left(\int_0^\infty g(0, R) R dR \right) / \left(\int_0^\infty g(0, R) dR \right), \quad (6)$$

where

$$g(t, \mathbf{R}) = \langle E(t' + t, \mathbf{R}' + \mathbf{R}) E(t', \mathbf{R}') \rangle / \langle E^2(t', \mathbf{R}') \rangle \quad (7)$$

is the coherence function¹⁸ of the PL signal $E(t, \mathbf{R})$ emitted by excitons and collected by the described system. In writing this formula we assumed, for convenience, that the second magnification (M_2) of the image occurs before the MZ interferometer, in which case \mathbf{R} is the coordinate in the plane of the fully magnified image.

Equation (5) is natural because an experimental measurement of any length is affected by the spatial resolution limit. However, such a limit always carries a numerical coefficient specific to the particular experimental technique (the difference between Abbe’s and Rayleigh’s formulas being an example). Our Eq. (5) shows that for ξ_x measured using the setup depicted in Fig. 1a, the Abbe limit must be divided by π . This makes its effect quantitatively smaller than one would naively think. For example, in our case² where $\text{NA} = \sin 16^\circ \approx 0.3$, the difference between ξ and ξ_x computed according to Eq. (5) (as well as by a more accurate approach presented below) is insignificant for all but a few data points at the boundary of the experimental resolution, see Fig. 2. Therefore, the case for a rapid and strong onset of the spontaneous coherence of the exciton gas below the temperature of a few degrees K remains intact.

In addition to the limitation from below, $\xi_x \gtrsim 1/Q$, the accuracy of the present method is restricted from above. When the coherence length exceeds the size of the studied region of the sample D/M_1 , the dependence of V on ξ_x should saturate, see Fig. 3. This may become important at low enough temperatures. The two limitations are indicated by the shaded areas in Fig. 2.

The remainder of the paper is organized as follows. In Sec. II we review the theoretical model used in our previous publication.² In Sec. III we refine it to incorporate the finite-resolution effects and derive Eq. (5). Discussion and conclusions are given in Sec. IV.

II. GEOMETRICAL OPTICS APPROACH

In order to construct the model of the described above measurement scheme, we need to know the functional form of $\rho(r)$. Unfortunately, at present there is no comprehensive theoretical framework that provides that. This is because $\rho(r)$ is affected by many factors, including thermal broadening and a variety of scattering mechanisms, see more in Sec. IV. On the other hand, the present state of experiment² does not allow us to extract reliably anything more than a characteristic decay length of function $\rho(r)$. Therefore, we take a pragmatic approach and approximate $\rho(r)$ by a simple exponential

$$\rho(r) = \rho(0) \exp(-r/\xi_x). \quad (8)$$

This *ansatz* should be reasonable over at least some range of r determined by the interplay of the disorder-limited mean-free path ($\sim 1 \mu\text{m}$ in high-mobility GaAs structures), thermal wavelength $\lambda_{\text{dB}} \sim 0.1 \mu\text{m}$, and possibly, some others. Most importantly, Eq. (8) provides a convenient starting point because it contains a single characteristic length ξ_x .

The crucial point is the relation between $\rho(r)$ and $g(R)$. If the experimental apparatus can be described by geometrical optics, then the only difference between the two functions is the linear magnification M and rescaling by

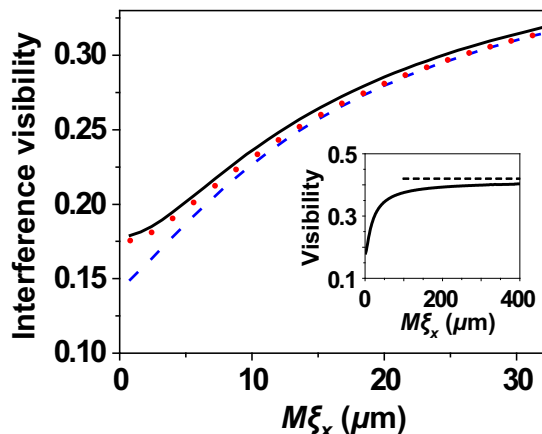


FIG. 3: Visibility of the interference fringes *vs.* ξ_x for parameters $\delta l = 4.2 \text{ mm}$, $D = 50 \mu\text{m}$, $M_1 = 5$, $M_2 = 1.6$, $Q^{-1} = 0.42 \mu\text{m}$. The solid line is the current theory; the dashed line is from Ref. 2; the dotted line is obtained from the dashed one by the replacement $\xi_x \rightarrow \sqrt{\xi_x^2 + Q^{-2}}$. The inset shows function $V(\xi_x)$ over a larger range of ξ_x , with the dashed line indicating the asymptotic value $V(\xi_x = \infty)$.

a constant factor. In this case, Eq. (8) entails

$$g(0, R) = g(0, 0) \exp(-R/M\xi_x). \quad (9)$$

In turn, Eq. (6) gives $\xi = \xi_x$, as expected. Until the very end of this section we will use these two lengths interchangeably.

We have shown previously² that the interference visibility contrast V is related to g as follows:

$$V = \frac{\theta(1-\Delta) \int_0^1 \frac{dz}{z} \sin[F(1-\Delta)z] \sin[F\Delta(1-z)] G(z)}{F\Delta \int_0^1 \frac{dz}{z} \sin(Fz)(1-z)G(z)}, \quad (10)$$

$$F = \pi \frac{AND_s}{\lambda_0}, \quad G(z) = g(0, zD_s), \quad \Delta = \frac{\delta l}{N\lambda_0},$$

where $\theta(z)$ is the step-function,¹⁹ $D_s = M_2 D$ is the fully magnified image of the pinhole diameter, A is the linear dispersion of the spectrometer, and N is the number of grooves in the diffraction grating. ($A = 1.55 \text{ nm/mm}$ and $N = 1.5 \times 10^4$ in Ref. 2.)

For g given by Eq. (9) it is straightforward to compute the integrals in Eq. (10); however, in general it has to be done numerically. For short coherence lengths, $\xi \ll \lambda_0/ANM, D_s/M$, one can also derive the analytical formula²

$$V \simeq \left(1 - \frac{\delta l}{N\lambda_0}\right) \left| \frac{\sin \pi X}{\pi X} \right|, \quad (11)$$

where

$$X = \frac{\delta l}{\delta l_0} \left(1 - \frac{M}{D_s} \xi\right), \quad \delta l_0 = \frac{\lambda_0^2}{AD_s}. \quad (12)$$

This equation can be obtained by expanding the sin-factors in the integrals to the order $\mathcal{O}(z)$ and extending their integration limits to infinity.

At $\delta l = \delta l_0$ and for small enough ξ , Eq. (11) yields

$$V(\delta l_0, \xi) \simeq \left(1 - \frac{\lambda_0}{AND_s}\right) \frac{M}{D_s} \xi. \quad (13)$$

Thus, as such δl the visibility contrast V vanishes unless ξ is nonzero. Working with $\delta l \approx \delta l_0$ ensures the highest sensitivity to ξ . In our experiment,² we extracted ξ at $\delta l = 4.2 \text{ mm}$, which is close but not exactly equal to $\delta l_0 = 5.2 \text{ mm}$. Therefore, we computed V using the full formula (10). The results are shown by the dashed line in Fig. 3. We fitted this theoretical curve $V(\xi)$ to the experimentally measured $V(T)$ (Fig. 2, upper inset) using $\xi = \xi(T)$ as an adjustable parameter. In this manner we obtain the graph shown by the squares in the main panel of Fig. 2. We see that the exciton coherence length exhibits a dramatic enhancement at $T < 4 \text{ K}$. On the other hand, at $T \sim 4 \text{ K}$ this approach gives $\xi_x = \xi \sim \lambda_0$. One can anticipate that the geometrical optics becomes inaccurate at such small ξ , so that ξ and ξ_x are in fact different. This question is studied in the next section.

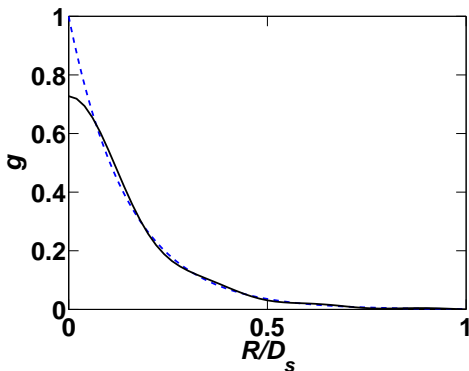


FIG. 4: Optical coherence function $g = g(0, R)$. The solid line is computed for the following set of parameters: $\xi_x = 1.5 \mu\text{m}$, $M = 8$, $Q^{-1} = 0.42 \mu\text{m}$, and $D_s = 80 \mu\text{m}$. The dashed line is for geometrical optics, $Q^{-1} = 0$.

III. DIFFRACTION EFFECTS

The conventional theory¹⁸ of the image formation in optical instruments laid down by Abbe¹⁵ in 1873 predicts that a point source imaged by a lens with a magnification M creates the diffraction spot

$$E(R) \propto \int_{k < Q} \frac{d^2k}{(2\pi)^2} e^{i\mathbf{k}\mathbf{R}/M} = \frac{2MQ}{R} J_1\left(\frac{QR}{M}\right) \quad (14)$$

in the image plane. Here R is the radial distance, Q is given by Eq. (5), and $J_1(z)$ is the Bessel function. The field distribution (14) is known as the Airy diffraction pattern.²⁰ The physical meaning of Q is the largest tangential wavenumber admitted by the lens. Accordingly, the diffraction can be alternatively viewed as a low-pass filtering of the incoming light by the lens.¹⁶

The Airy pattern plays the role of the response function of the lens. Its finite spread in R imposes the limit on the achievable optical resolution $\sim Q^{-1}$ and is the source of the difference between the optical and the actual exciton coherence lengths, see Eq. (5). Indeed, because of the diffraction, the coherence function $g(R)$ is not just a rescaled copy of $\rho(R/M)$ but its convolution with the Airy pattern. Using tilde to denote the 2D Fourier transform, we can express this fact as follows:

$$\tilde{g}(k) \propto \theta(Q - Mk) \tilde{\rho}(Mk). \quad (15)$$

As mentioned earlier, $\tilde{\rho}(k)$ has the physical meaning of the momentum occupation function for excitons. Computing this $\tilde{\rho}(k)$ from Eq. (8), we get

$$\tilde{g}(k) = \text{const} \times \frac{\theta(Q - Mk)}{(1 + M^2 \xi_x^2 k^2)^{3/2}}. \quad (16)$$

The constant prefactor in this formula has no effect on V . It is convenient to choose it to be $2\pi M^2 \xi_x^2$, so that

$$g(0, R) = M^2 \xi_x^2 \int_0^{Q/M} \frac{J_0(kR) k dk}{(1 + M^2 \xi_x^2 k^2)^{3/2}}. \quad (17)$$

In this case in the limit $Q \rightarrow \infty$, we recover Eq. (9) with $g(0, 0) = 1$. On the other hand, for finite Q , we have

$$g(0, 0) = 1 - \frac{1}{\sqrt{1 + Q^2 \xi_x^2}}. \quad (18)$$

Additionally, at large R , function $g(0, R)$ acquires the behavior characteristic of the Airy pattern (14): quasiperiodic oscillations with the envelope decaying as $R^{-3/2}$, see Fig. 4. Finally, computing the optical coherence length ξ according to Eq. (6) we get Eq. (5).

The refined theoretical dependence of V on ξ_x can now be obtained by substituting Eq. (17) into Eq. (10). As before, for small ξ_x analytical formulas (11)–(13) suffice, with ξ defined by Eq. (5). When this ξ becomes comparable to D_s/M , numerical evaluation of Eqs. (10) and (17) is necessary. The representative results are shown by the solid line in Fig. 3. For comparison, two other curves are included. The dashed line is the geometrical optics approximation, $\xi = \xi_x$ of Sec. II. The dotted line is the result of correcting the latter according to Eq. (5) and using Q appropriate for our experiment. As one can see, at small ξ_x , the effect of the diffraction-limited resolution of the optical system is indeed accounted for by Eq. (5). At large ξ_x , the correction becomes small and all the curves are very close to each other.

It is instructive to examine how our conclusions so far depend on the model assumption (8) about function $\rho(r)$. For example, let us replace this exponential *ansatz* by the Gaussian one,

$$\rho \propto \exp\left(-\frac{r^2}{\pi \xi_x^2}\right), \quad \tilde{\rho}(k) = \tilde{\rho}(0) \exp\left(-\frac{\pi}{4} k^2 \xi_x^2\right). \quad (19)$$

This is similar to Maxwell-Boltzmann distribution except the coefficients in the exponential factors are adjusted to satisfy Eq. (2). Let us compute the corresponding ξ . Using Eq. (15), we can rewrite Eq. (6) as follows:

$$\xi = \tilde{\rho}(0) / \left(\int_0^Q dk \tilde{\rho}(k) \right), \quad (20)$$

Substituting here $\tilde{\rho}(k)$ from Eq. (19), we get

$$\xi = \frac{\xi_x}{\text{erf}[(\sqrt{\pi}/2)Q\xi_x]}, \quad (21)$$

where $\text{erf}(z)$ is the error function. This formula replaces Eq. (5). Interestingly, it implies that for the same ξ_x and Q , the effect of the finite resolution in the case of a Gaussian decay is always smaller than for the exponential one. The direct numerical evaluation of Eq. (10) with the Gaussian profile (19) confirms this expectation, see Fig. 5. Thus, we again conclude that the diffraction correction is important for $\xi \lesssim \lambda_0$, but it is very small in the most interesting low-temperature region $T < 4\text{K}$ where $\xi > \lambda_0$.

Notice that function $V(\xi_x)$ increases somewhat faster with ξ_x for the Gaussian case compared to the exponential one, cf. Figs. 3 vs. 5. Therefore, had we adopted

the Gaussian *ansatz* (19), the deduced values of $\xi_x(T)$ would have been somewhat smaller than those plotted in Fig. 2. This is to be expected: if the exact functional form of $\rho(r)$ is unknown, its characteristic decay length can be determined only up to a numerical coefficient of the order of unity.

IV. DISCUSSION

The main purpose of the present work is refinement of the optical method for determining the one-body density matrix $\rho(r)$ of excitons. We showed that in order to obtain the characteristic decay length ξ_x of $\rho(r)$, the optical coherence length ξ of the exciton emission should be corrected because of the diffraction-limited spatial resolution of the experimental apparatus. However the correction is insignificant as long as ξ_x is larger than about one wavelength and the numerical aperture NA of the experimental setup is not too small. The correction does grow as NA decreases, and so reduced NA should be avoided.

It is well known^{15,16,18} that limitation of the spatial resolution due to diffraction is equivalent to that due to restriction on tangential wavenumbers k admitted by the lens collecting the signal. This k -filtering effect has been considered in Ref. 21 in application to the measurements of the exciton coherence length. For the collection angle $\alpha = 16^\circ$ in our experiments,² the results presented in Fig. 3c of Ref. 21 give the correlation length due to the k -filtering effect $\xi_\gamma \approx 1 \mu\text{m}$. (This length plays the role similar to that of $Q^{-1} = 0.42 \mu\text{m}$ in our formalism.) For the considered $\rho(r)$ this correction enters either through the quadratic sum, Eq. (5), or the error function, Eq. (21). As a result, the estimation of the k -filtering effect per Ref. 21 gives only a small ($\sim 10\%$) correction,

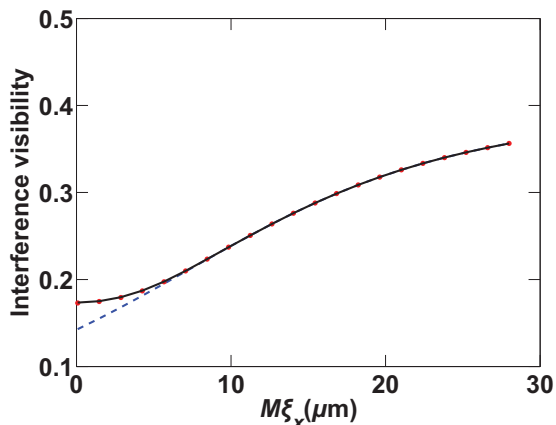


FIG. 5: Visibility of the interference fringes *vs.* ξ_x for the Gaussian coherence function (19) and the parameters of Fig. 3. The solid line includes the diffraction correction; the dashed line is for the geometrical optics; the dotted line is obtained from the dashed one by the replacement of ξ_x by ξ according to Eq. (21).

e.g., $\xi - \sqrt{\xi^2 - \xi_\gamma^2}$ to the optical coherence length ξ mea-

sured in Ref. 2 at low T . Therefore, it cannot explain the observed large enhancement of the coherence length at $T < 4$ K. Our calculations indicate that the correction is even smaller.

The discussion of physics that is responsible for the observed rapid change in $\rho(r)$ at low temperatures is however beyond the scope of this paper. As a final word, we would like to offer only the following minimal remarks on this matter.

Function $\rho(r)$ is influenced by a number of factors, including Bose statistics, interactions, and scattering. The effect of the first two has been studied extensively, albeit for simplified models of interaction. According to present understanding,^{4,5} the long-distance behavior of function $\rho(r)$ is qualitatively different above and below the Berezinskii-Kosterlitz-Thouless (BKT) transition temperature T_{BKT} . At $T \gg T_{\text{BKT}}$, where $\tilde{\rho}(k)$ obeys the classical Boltzmann statistics, $\rho(r)$ decays as a Gaussian, Eq. (19), with the coherence length

$$\xi_x = \lambda_{\text{dB}}/\pi. \quad (22)$$

[Our estimates of ξ_x at $T < 4$ K exceed λ_{dB}/π by an order of magnitude, suggesting that Eq. (22) does not apply at such temperatures.] At $T < T_{\text{BKT}}$, the eventual asymptotic decay of the density matrix becomes algebraic, $\rho(r) \propto r^{-\nu}$ with a temperature-dependent exponent $\nu(T)$. The behavior of $\rho(r)$ at intermediate temperatures and/or distances is more complicated. In general, it can be computed only numerically, e.g., by quantum Monte-Carlo method.⁵

Some of the other mechanisms of limiting the coherence length ξ_x , such as exciton recombination and exciton-phonon scattering are too weak to significantly affect the large magnitude of observed ξ_x at low temperatures.² However, scattering by impurities and defects should be seriously considered. It can substantially modify the functional form of $\rho(r)$ compared to the disorder-free case. Indeed, weak disorder typically leads to an exponential decay of the correlation functions on the scale of the mean-free path, which in fact inspired our *ansatz* (8). As temperature goes down, the strength of the disorder decreases because excitons can screen it more efficiently.^{22,23,27} This should increase both the mean-free path and the exciton coherence length.

The comprehensive theoretical calculation of the exciton coherence length that would take into account all relevant thermal, interaction, and disorder screening effects is yet unavailable.

Acknowledgments

We thank A. Ivanov and L. Mouchliadis for valuable discussions and comments on the manuscript. This work is supported by NSF grants DMR-0606543, DMR-0706654, and ARO grant W911NF-05-1-0527.

-
- ¹ G. D. Mahan, *Many Particle Physics*, 3rd ed. (Springer, Berlin, 2000).
- ² S. Yang, A. T. Hammack, M. M. Fogler, and L. V. Butov, *Phys. Rev. Lett.* **97**, 187402 (2006).
- ³ L. V. Butov, *J. Phys.: Condens. Matter* **16**, R1577 (2004).
- ⁴ V. N. Popov, *Functional Integrals in Quantum Field Theory and Statistical Physics* (Reidel, Dordrecht, 1983).
- ⁵ Yu. Kagan, V. A. Kashurnikov, A. V. Krasavin, N. V. Prokof'ev, and B. V. Svistunov, *Phys. Rev. A* **61**, 043608 (2000).
- ⁶ Th. Östereich, T. Portengen, and L. J. Sham, *Solid State Commun.* **100**, 325 (1996).
- ⁷ B. Laikhtman, *Europhys. Lett.* **43**, 53 (1998).
- ⁸ A. Olaya-Castro, F. J. Rodriguez, L. Quiroga, and C. Tejedor, *Phys. Rev. Lett.* **87**, 246403 (2001).
- ⁹ R. Zimmermann, *Solid State Commun.* **134**, 43 (2005).
- ¹⁰ L. V. Butov, A. C. Gossard, and D. S. Chemla, *ArXiv:cond-mat/0204482*; *Nature (London)* **418**, 751 (2002).
- ¹¹ Here we remedy an error in handling parameter M_2 in the previous paper.² Therein $M_2 = 1.6$ was determined from the data analysis. However, by confusion the estimated value of $M\xi$ was divided by $M = 10$ (instead of $M = 5 \times 1.6 = 8$) to give the result for ξ . Accordingly, the values of ξ in Fig. 3e of Ref. 2 are somewhat smaller than what should have been shown. (For ease of comparison, this figure is reproduced in the lower inset of Fig. 2.) In the main panel of Fig. 2 and the rest of the present paper this error has been corrected: we use $M_2 = 1.6$ and $M = 8$ throughout.
- ¹² D. S. Fisher and P. C. Hohenberg, *Phys. Rev. B* **37**, 4936 (1988).
- ¹³ N. Prokof'ev and B. Svistunov, *Phys. Rev. A* **66**, 043608 (2002).
- ¹⁴ Exciton concentration n can be deduced from the exciton energy $E_x = hc/\lambda_0$ using the linear relation $n = (C/e^2)[E_x - E_x(n = 0)]$. However, the value of the coefficient C is presently under debate. Earlier literature^{24,25,26,27} assumed that C is equal to the classical capacitance per unit area $C = \epsilon/(4\pi d)$, where ϵ is the dielectric constant and d is the separation between the electron and hole layers. A more recent calculation²⁸ gives an order of magnitude higher estimate for C and therefore n in our experiments.
- ¹⁵ E. Abbe, *Arch. f. Mikroskop. Anat.* **9**, 413 (1873).
- ¹⁶ H. Köhler, *J. Mod. Opt.* **28**, 1691 (1981).
- ¹⁷ L. Rayleigh, *Mon. Notes Roy. Astron. Soc.* **33** 59 (1872). Reprinted in L. Rayleigh, *Scientific Papers* (Dover, New York, 1964), Vol. I, p. 163.
- ¹⁸ M. Born and E. Wolf, *Principles of Optics*, 7th ed. (Cambridge University Press, Cambridge, UK, 1999).
- ¹⁹ The absence of “ θ ” and the extra “sin” in the corresponding Eq. (7) of Ref. 2 are typographic errors.
- ²⁰ G. B. Airy, *Phil. Mag. Ser. 3* **18**, 1 (1841). The Airy formula is actually not exact but it is a good approximation near the optical axis, see J. D. Jackson, *Classical Electrodynamics* (Wiley, New York, 1998).
- ²¹ L. Mouchliadis and A. L. Ivanov, *arXiv:0802.4454*.
- ²² L. V. Butov and A. I. Filin, *Phys. Rev. B* **58**, 1980 (1998).
- ²³ D. E. Nikonov and A. Imamoglu, *ArXiv:quant-ph/9806003*.
- ²⁴ D. Yoshioka and A. H. MacDonald, *J. Phys. Soc. Jpn.* **59**, 4211 (1990).
- ²⁵ X. Zhu, P. B. Littlewood, M. Hybertsen, and T. M. Rice, *Phys. Rev. Lett.* **74**, 1633 (1995).
- ²⁶ Yu. E. Lozovik and O. L. Berman, *JETP Lett.* **64**, 573 (1996).
- ²⁷ A. L. Ivanov, *Europhys. Lett.* **59**, 586 (2002).
- ²⁸ C. Schindler and R. Zimmermann, *arXiv:0802.3337*.